Acta Biochimica Polonica

Vol. 51 No. 1/2004

33–49

QUARTERLY

Review

Solution structure of conformationally restricted vasopressin analogues★✪

Emilia Trzepałka[1]✉, Marta Oleszczuk[2], Maciej Maciejczyk[2] and Bernard Lammek[1]

[1]*Faculty of Chemistry, University of Gdańsk, Gdańsk, Poland;* [2]*Laboratory of Biological NMR, Institute of Biochemistry and Biophysics, Polish Academy of Sciences, Warszawa, Poland*

Received: 31 October, 2003; revised: 04 February, 2004; accepted: 08 February, 2004

Key words: EDMC, NMR spectroscopy, peptide conformation, vasopressin, X-PLOR

In recent years, a massive effort has been directed towards designing potent and selective antagonists of neurohypophyseal hormones substituted at position 3. Modification of vasopressin at position 3 with 4,4′-biphenylalanine results in pharmacologically inactive analogues. Chemically, this substitution appears to vary only slightly from those previously made by us (1-Nal or 2-Nal), which afforded potent agonists of V_2 receptors. In this situation, it seemed worthwhile to study the structure of the analogues with 4,4′-biphenylalanine (BPhe) at position 3 in aqueous solution using NMR spectroscopy and total conformational analysis. This contribution is part of extensive studies aimed at understanding spatial structures of 3-substituted [Arg^8]vasopressin analogues of different pharmacological properties. NMR data were used to calculate 3D structures for all the analogues using two methods, EDMC with the ECEPP/3 force field, and molecular dynamic with the simulated annealing (SA) algorithm. The structures obtained by the first method show a better fit between the NMR spectral evidence and the calculation for all the peptides.

✪Presented at the 17th Polish Peptide Symposium, August 31st–September 4th, 2003, Łódź, Poland.

✪This work was supported in part by the State Committee for Scientific Research (KBN, Poland), grant No. 0863/T09/2002/22.

✉Correspondence to: Emilia Trzepałka, Faculty of Chemistry, University of Gdańsk, J. Sobieskiego 18, 80-952 Gdańsk, Poland; e-mail: milka@chemik.chem.univ.gda.pl

Abbreviations: AVP, [Arg^8]vasopressin; BPhe, 4,4′-biphenylalanine; Cpa, 3-mercapto-3,3-cyclopentamethylenepropionic acid; 2D, two-dimensional; DSS, 2,2-dimethyl-2-silapentane-sulfonic acid; ECEPP/3, empirical conformational energy program for peptides; EDMC, electrostatically driven Monte Carlo; MORASS, multiple Overhauser relaxation analysis and simulation; 2-Nal, L-3-(2-naphthyl)-alanine; 1-Nal, L-3-(1-naphthyl)-alanine; RMSD, the root mean square deviation; SA, simulated annealing; SRFOPT, solvent-accessible surface model.

[Arg^8]vasopressin (AVP) plays a primary role in the regulation of renal water excretion and a secondary role in the regulation of cardiovascular function in mammals. Agonists and antagonists of this hormone have been widely noted in studies aimed at clarifying the role of endogenous vasopressin in a variety of physiological and pathophysiological conditions. Moreover, one of the agonists of antidiuretic responses to AVP (agonist of V_2 receptors), namely 1-desamino-8-D-arginine vasopressin (dDAVP), is now a drug of choice for the treatment of diabetes insipidus. It is also worth mentioning that antagonists of V_2 receptors have a potential as therapeutic agents for the treatment of hyponatraemia, secondary to the syndrom of inappropriate secretion of the antidiuretic hormone (SIADH) (Langfeldt & Cooley, 2003).

The importance of AVP analogues has prompted many scientists to synthesize thousands of new peptides to establish a structure–activity relationship aimed at the development of either selectively active analogues or those with a sustained effect. However, the design of peptides that are truly selective for V_{1a}, V_2 and other AVP receptors remains a challenge.

Both NMR and theoretical methods are often very useful in examining the conformations of the hormones and their analogues, they can thus provide good tools in the effort to better correlate the relations between structure and activity of the peptides.

In recent years, a massive effort has been directed towards designing potent and selective antagonists of neurohypophyseal hormones substituted at position 3. Until recently, the Phe group at position 3 was thought to be crucial for producing agonism both towards the V_2 and V_{1a} receptors (Manning *et al.*, 1997; Hlavacek, 1987). However, this assumption has been questioned by new reports indicating that substitution of the Phe^3 residue by conformationally restricted and bulky aromatic amino acids might result in analogues of interesting pharmacological properties (Manning *et al.*, 1997; Stoev *et al.*, 1999). An additional stimulus to continue these efforts was provided by the results of research carried out in our laboratory, which demonstrated that substitution at position 3 of dDAVP of either the L-3-(2-naphthyl)-alanine (2-Nal) or L-3-(1-naphthyl)-alanine (1-Nal) residues afforded potent agonists of V_2 receptors. In addition, the [Mpa^1, (1-Nal)^3, (D-Arg)^8]VP analogue was distinguished by its high selectivity (Lammek *et al.*, 1997). These encouraging findings prompted us to design and synthesize three further analogues of vasopressin modified at position 3 with an aromatic residue restricting the conformational freedom of the molecule, namely with 4,4′-biphenylalanine (BPhe) (Fig. 1).

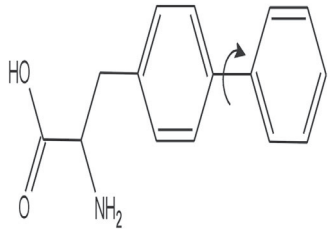

Figure 1. Structure of 4,4′-biphenylalanine.

Furthermore, in one of the peptides the modification was extended by changing the conformation of the Arg^8 residue, and in another, 3-mercapto-3,3-cyclopentamethylenepropionic acid (Cpa) was substituted at position 1 (Scheme 1). These modifications were

$\overline{\text{Cys-Tyr-BPhe-Gln-Asn-Cys}}$-Pro-Arg-Gly-$NH_2$, [BPhe^3]AVP;

$\overline{\text{Cys-Tyr-BPhe-Gln-Asn-Cys}}$-Pro-D-Arg-Gly-$NH_2$, [BPhe^3, D-AVP^8]VP;

$\overline{\text{Cpa-Tyr-BPhe-Gln-Asn-Cys}}$-Pro-Arg-Gly-$NH_2$, [Cpa^1, BPhe^3]AVP.

Scheme 1

based on the findings that substitution of the acid enhances the antagonistic efficacy of the analogues (Manning *et al.*, 1987; László *et al.*, 1991), while the change of configuration of Arg^8 evokes antidiuretic activity and/or selectivity of action (Manning *et al.*, 1976).

The results of biological experiments showed that modification of [Arg^8]AVP at position 3 with BPhe results in pharmacologically inactive analogues (Trzeciak, unpublished). Again, from the chemical standpoint, the substitution with BPhe appears to be only a slight variation of those previously made by us (1-Nal or 2-Nal). It has, however, a dramatic influence on the biological activity of the peptides. In this situation, it seemed worthwhile to study the structures of these analogues in aqueous solution, utilizing 2D NMR spectroscopy supplemented with two different computational methods. The present contribution is a part of extensive studies aimed at understanding the spatial structures of 3-substituted AVP analogues of different pharmacological properties. We believe that the understanding the differences in the structure would contribute to designing peptides with definite pharmacological properties.

NMR MEASUREMENTS

NMR spectra were recorded on a 500 MHz VARIAN and a 600 MHz DMX BRUKER spectrometer. The experiments were carried out in H_2O/D_2O (9:1). The sample concentration was approximately 7 mM in 0.5 ml of H_2O/D_2O, pH = 4.9 for the [BPhe^3]AVP and [BPhe^3, D-AVP^8]VP peptides and pH = 5.1 for the [Cpa^1, BPhe^3]AVP peptide. All spectra were recorded at 298 K except for those for the temperature coefficients of the amide protons chemical shifts, measured over the range of 275–323 K.

The assignment of proton chemical shifts of the three peptides was accomplished using the proton-proton total chemical shift correlation spectroscopy (TOCSY) (Bax & Davis, 1985b; Braunschweiler & Ernst, 1983), the rotating-frame Overhauser enhancement spectroscopy (ROESY) (Bax & Davis, 1985a), as well as the gradient heteronuclear single quantum coherence (^{1}H-^{13}C gHSQC, ^{1}H-^{15}N gHSQC) (Palmer *et al.*, 1991; Kay *et al.*, 1992; Kontrais *et al.*, 1994). For each peptide, the mixing times of 70 ms and 250 for TOCSY and ROESY, respectively, were used. Spectral processing was carried out using NMRPipe/NMRDraw (Delaglio *et al.*, 1995) and analyzed with XEASY (Bartles *et al.*, 1995). The spectra were calibrated against the HDO signal, taking into account the temperature drift of the reference signal given by the equation $\delta_{1H(T)} = 5.060 - 0.0122T + (2.11 \times 10^{-5})T^2$, T[°C] (Gottlieb *et al.*, 1997). External reference signals used for calibration of the correlation spectra were those of DSS (2,2-dimethyl-2-silapentanesulfonic acid) for the carbon axis in the ^{1}H-^{13}C spectra (^{13}C/^{1}H = 0.251449530) and the NH_3 signal for the nitrogen axis in the ^{1}H-^{15}N spectra (^{15}N/^{1}H = 0.101329118) (Wishart *et al.*, 1995).

The analysis of the residual spin-coupling correlation systems was straightforward, being performed by a combination of the sequential-specific assignment procedure in the TOCSY and the sequential ROE network along the peptide backbone protons (Tables 1–3). The positions of H_β and H_γ protons of Pro^7 for each analogue and the protons of Cpa^1 were found in the ^{1}H-^{13}C gHSQC spectra. On the basis of the ^{1}H-^{15}N gHSQC spectra, the chemical shifts of ε-NH_2 protons of Gln^4 and δ-NH_2 of Asn^5 for each peptide and H_N of BPhe^3 of [Cpa^1, BPhe^3]AVP were marked. All the ROE cross-peaks for all peptides were picked up on the ROESY spectra with mixing time of 250 ms. The value of the temperature dependence of H_N proton chemical shifts ($\Delta\delta/\Delta T$) was calculated from the 1D spectra recorded at 275, 283, 293, 303, 313 and 323 K.

The coupling constants between H_α and H_N ($^3J_{HNH\alpha}$) were found in the ACT-ct-COSY (Koźmiński, 1998) and 1D NMR spectra. The error delimitation of the values of coupling constants was 0.1–0.5 Hz.

CONFORMATIONAL CALCULATIONS

The conformational space of each peptide was determined using two methods, EDMC (Ripoll & Scheraga, 1988) with the ECEPP/3 force field (Némethy *et al.*, 1992) and molecular dynamic with the simulated annealing (SA) algorithm.

In the first method, the applied algorithm consists of the following three steps: (i) search of the conformational space in order to find conformations with reasonably low energy, (ii) simulation of the NOE spectrum and vicinal coupling constants for each of the low energy conformations, and (iii) determining the statistical weights of the conformations, by means of the maximum entropy method in order to obtain the best fit of the averaged NOE intensities and coupling constants to the experimental quantities (Groth *et al.*, 1999).

In the second method, the structure calculation was performed using the X-PLOR program (Brünger, 1992). The algorithm SA was used for each peptide. According to the NMR data, the inter-proton distances were calculated by the CALIBA algorithm and the torsion angles were computed by the HABAS algorithm of the DYANA program (Güntert & Wüthrich, 1991) on the basis of the Bystrov–Karplus equation (Bystrov, 1976).

The β-turn types and positions detected in the calculated conformations were defined according to Lewis *et al.* (1973). For displaying and analyzing the three-dimensional structure of vasopressin analogues the molecular graphics MOLMOL program (Koradi *et al.*, 1996) was used. The hydrogen bonds were calculated using the HBPLUS (McDonald & Thornton, 1994) program (the hydrogen-acceptor distance (H-A) criterion was ≤2.5 Å, the donor-acceptor (D-A) distance criterion was ≤3.9 Å and the donor-hydrogen-acceptor angle (DHA) criterion was ≥90°).

THE EDMC AND ANALYZE CALCULATIONS

A global conformational search of the peptides studied was carried out using the Electrostatically Driven Monte Carlo (EDMC) method (Ripoll & Scheraga, 1988) with the ECEPP/3 force field (Némethy *et al.*, 1992), which assumes rigid valence geometry. The force field included a hydration contribution, which was evaluated in the SRFOPT solvent-accessible surface model (Vila *et al.*, 1991), whose parameters pertain to solvation by water. According to the NMR data, the chirality of all C_α atoms (except that of residue Arg^8 of the peptide [$BPhe^3$, D-Arg]VP) was fixed to the L configuration. A total of 3000 energy-minimized conformations were generated for each peptide. The working temperature was 1000 K. The conformations were subsequently clustered into families using the minimum-variance algorithm (Späth, 1980). The root mean square deviation (RMSD) between heavy atoms at the optimal superposition was taken as the measure of the distance between conformations, and a cut-off value of 1.4 Å was used to separate the families to afford 981, 414 and 783 families of conformations for [$BPhe^3$]AVP, [$BPhe^3$, D-Arg^8]VP and [Cpa^1, $BPhe^3$]AVP, respectively.

In the next step, for the lowest energy conformation of each family, a NOESY spectrum and vicinal constants coupling, $^3J_{HNH\alpha}$, were calculated by using the MORASS (Meadows *et al.*, 1994; Post *et al.*, 1990) program. This program solves the system of Bloch differential equations (Massefski & Bolton, 1985) for the cross-relaxation of a system of interacting proton spins. The vicinal couplings, $^3J_{HNH\alpha}$, were calculated from the empirical Bystrov–Karplus relationship (Bystrov, 1976). The NOE effects were generated using a correlation time of 0.45 ms (Yu *et al.*, 1992), mix-

ing time of 250 ms and cut-off value of 6 Å. The weight of the coupling constant term was 0.5 in the minimized sum and the Marquardt convergence criterion (Marquardt, 1963) equal to 10^{-5} was used. The entropy factor, α = 0.2, was used for all peptides. The populations of the families were determined by fitting a linear combination of the generated spectra and coupling values to the experimental data.

The conformations with statistical weights greater than 4, 7 and 8% for [BPhe^3]AVP, [BPhe^3, D-Arg^8]VP and [Cpa^1, BPhe^3]AVP, respectively, were used in further analyses.

X-PLOR CALCULATIONS

The solution structures of the major species of each peptide studied were computed using the experimental: ROE inter-proton cross-peaks and vicinal coupling constants $^3J_{HNH\alpha}$. According to the NMR data, the inter-proton distances were calculated by the CALIBA algorithm of the DYANA program (Güntert & Wüthrich, 1991), which performs a standard calibration of the current peaks using three different calibration classes: one for ROE assigned to backbone protons, one for ROE assigned to the more flexible side-chain protons and one for ROE assigned to methyl groups. In the next step, by using the macro GRIDSEARCH with the command "distance modify", irrelevant constraints (constraints that involve fixed distances and constraints which cannot be violated) were removed, retaining maximally one distance limit for each atom pair and introducing corrections for constraints with diastereotopic substituents for which stereospecific assignments are not available (Wüthrich *et al.*, 1983; Güntert *et al.*, 1991). Torsion angles were calculated by the HABAS algorithm of the DYANA program (Güntert & Wüthrich, 1991), on the basis of the Bystrov–Karplus equation (Bystrov, 1976). In the next step, the standard modules of the XPLOR program (Brünger, 1992) were used. The simulating annealing (SA) algorithm was applied for each peptide. The geometry of the peptide groups (all *trans*; f = 500 kcal/mol · rad^2) was kept fixed. For each peptide, the chirality of all C_α atoms, except for the arginine residue in [BPhe^3, D-Arg]VP, were fixed to L. A simulated annealing protocol incorporating ambiguous distance restraints and floating chirality was used. Force constants f = 50 kcal/mol · Å^2 and f = 5 kcal/mol · rad^2 for the distance restraints and the dihedral angle restraints, respectively, were used during the simulation. The calculations were carried out using the CHARMM force field (Brooks *et al.*, 1993) *in vacuo*. Simulated annealing started from the template coordinate set. For each molecule 300 cycles of SA were carried out. Electrostatic interactions and energy of hydrogen bonds were not directly included. In each cycle, the molecule was heated to 2000 K and equilibrated at this temperature for 40 ps, then cooled down to 1000 K for 30 ps and finally cooled from 1000 K to 100 K for 15 ps. Finally, 500 iterations of energy minimization with the use of the Powell algorithm were performed. As a result, 300 energy-minimized conformations were obtained. Then, the sets of the final conformations were clustered (using the minimal-tree algorithm) for each peptide. The RMSD of all heavy atoms at the optimum superposition was taken as the measure of the distance between conformations, and the cut-off values of 2.4 Å for all peptides were used to separate the families.

NMR RESULTS

In this paper, the conformations of three analogues of vasopressin in aqueous solution were investigated by two-dimensional NMR spectroscopy. In particular, the influence of the substitution of Cys^1, Phe^3 and Arg^8 with 3-mercapto-3,3-cyclopentamethylenepropionic acid, 4,4′-biphenylalanine and D-Arg, respec-

tively, on the conformation and flexibility of the peptide was examined.

In the ROESY map, the following number of intraresidual, sequential and medium-range interactions for the [BPhe^3]AVP, [BPhe^3, D-Arg^8]VP and [Cpa^1, BPhe^3]AVP peptides, respectively, were identified: 56, 29 and 10; 56, 29 and 9; and 48, 25 and 10.

The observable NMR parameters are averaged over the entire conformational ensemble, but the characteristic NOE connectivities and temperature coefficients or coupling constants, $^3J_{HNH\alpha}$, which are diagnostic of reverse turns, are sufficient to identify even quite small populations of these structures (Dyson *et al.*, 1988). The sequential H_α(i) – H_N(i + 1) NOE connectivity is always observed and is mostly very strong. Much weaker H_β(i) – H_N(i + 1) connectivities are often found. Sequential H_N(i) – H_N(i + 1) NOE connectivities are seen only in those regions of peptides which preferentially adopt folded conformations. Intraresidual H_α(i) – H_N(i) and H_β(i) – H_N(i) NOE connectivities are also present for most peptides (Dyson *et al.*, 1988). In unfolded peptides, the H_α(i) – H_N(i) connectivity is much weaker than the sequential H_α(i) – H_N(i + 1) connectivity, despite the finding that the maximum value of the H_α(i) – H_N(i) distance is 2.8 Å (Wüthrich *et al.*, 1984).

Figure 2a shows the ROE effect patterns and vicinal couplings values, $^3J_{HNH\alpha}$, for the [BPhe^3]AVP peptide. The presence of H_N(4) – H_N(5) and H_N(5) – H_N(6) cross-peaks suggests that the β-turn is at position 4,5. The cross-peaks H_α(i) – H_N(i + 1) indicate the presence of β-turns at positions 2,3; 3,4; 4,5 and 7,8. Additional cross-peaks H_α(4) – H_N(6) confirms the β-turn at position 4,5. The small value of the $^3J_{HNH\alpha}$ coupling of residue 4 (3.9 Hz) and the higher value measured for residue 5 (8.5 Hz) suggest the presence of a β-turn at the 4,5 position. The small value of the temperature coefficient of the H_N of Cys^6 may be caused by the hydrogen bonding of this proton to oxygen atom of the carbonyl

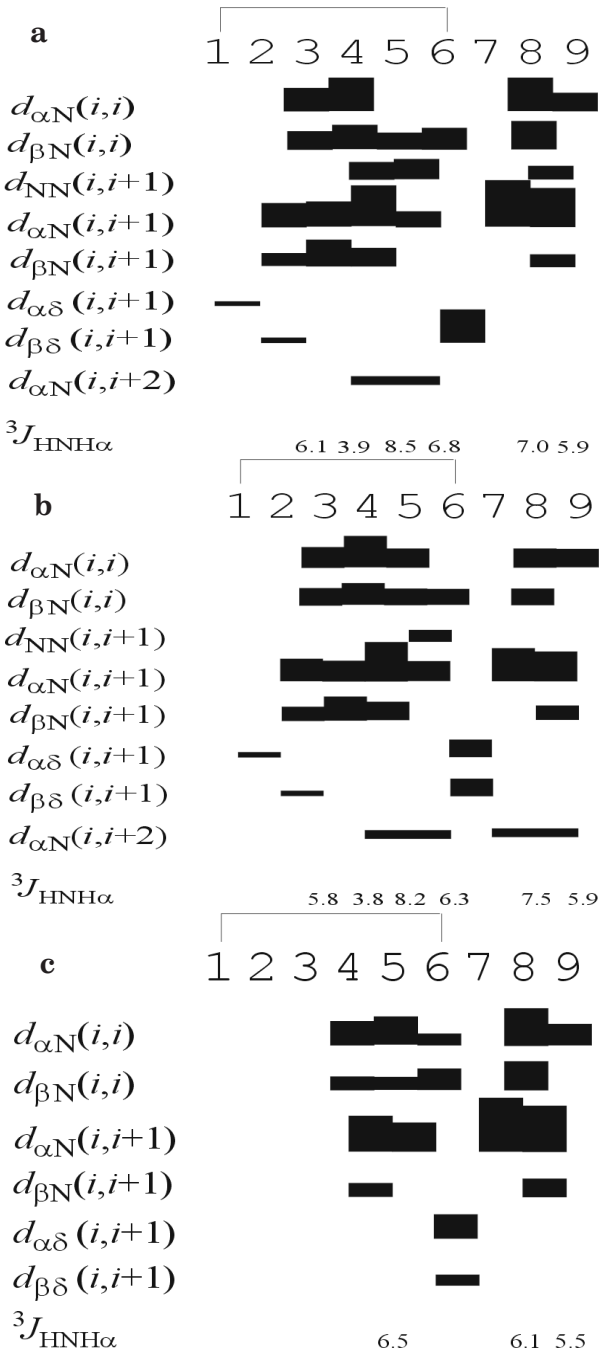

Figure 2. The ROE effects corresponding to the inter-proton distances and $^3J_{HNH\alpha}$ measured for the [BPhe^3]AVP (a), [BPhe^3, D-Arg^8]VP (b) and [Cpa^1, BPhe^3]AVP (c) peptides.

group of BPhe^3 (β-turn) or to the oxygen atom of the carbonyl group of Gln^4 (γ-turn).

Figure 2b summarizes the ROE patterns and vicinal couplings values $^3J_{HNH\alpha}$ for peptide [BPhe^3, D-Arg]VP. In this peptide, the H_α(i) – H_N(i + 1) and H_β(i) – H_N(i + 1) cross-peaks suggest that the β-turn at position 3,4 is

populated. On the basis of the $^3J_{HNH\alpha}$ coupling constants of residues 4 and 5 (3.8 Hz and 8.2 Hz, respectively) one can suggest the presence of a β-turn at position 4,5. The low temperature coefficient of the H_N of Gln^4 may be caused by the hydrogen bonding of this proton either to the oxygen atom of the carbonyl group of Cys^1 (β-turn) or to that of Phe^2 (γ-turn). A small coefficient was also found for the signal of the H_N proton of Cys^6, which may form a hydrogen bond to the oxygen atom of the carbonyl group of either $BPhe^3$ (β-turn) or Gln^4 (γ-turn).

For the [Cpa^1, $BPhe^3$]AVP analogue, a small number of ROE cross-peaks was noted. The $H_N(i) - H_N(i + 1)$ cross-peaks were missing. The cross-peaks of $H_\alpha(4) - H_N(5)$ and $H_\alpha(5) - H_N(6)$ seem to confirm the presence of the β-turn at position 4,5. The magnitudes of the $^3J_{HNH\alpha}$ couplings do not permit confirmation of the occurrence of β-turns (Fig. 2c). Large temperature coefficients of the H_N protons suggest an absence of hydrogen bonds.

For the [$BPhe^3$]AVP and [$BPhe^3$, D-Arg^8]VP analogues ROE cross-peaks between Cys^1 and Cys^6 residues were observed. The $H_\alpha Cys^1$ proton interacted with both H_β proton sites of the Cys^6 residues, while the $H_\alpha Cys^6$ proton did not show any correlation with $H_\beta Cys^1$. This result unambiguously revealed the preference of the conformation in which the S-S dihedral angle was confined to a negative value of approximately −90° (Schmidt *et al.*, 1991).

In the ROESY spectra of the [$BPhe^3$, D-Arg^8]VP and [Cpa^1, $BPhe^3$]AVP peptides, the presence of the cross-peaks of $H_\alpha Cys^6$ and

Table 1. Proton and carbon chemical shifts [p.p.m.] and the amide proton temperature coefficients [ppb/K] of the [$BPhe^3$]AVP peptide in water at 25°C

Residue	Chemical shift [ppm]						$-\Delta\delta/\Delta T$
	H_N	$C_\alpha H$	$C_\beta H$	$C_\gamma H$	$C_\delta H$	Others	[ppb/K]
Cys^1	n. o.	4.14 55.52	3.31; 3.13 42.66				n. o.
Tyr^2	n. o.	4.64 n. o.	2.94; 2.87 39.07			$H_{2,6}$ 7.03; $H_{3,5}$ 6.79 $C_{2,6}$ 131.13; $C_{3,5}$ 116.34	n. o.
$BPhe^3$	7.92	4.57 n. o.	3.24; 3.08 36.79			$H_{2,6}$ 7.23; $H_{3,5}$ 7.63 $H_{2',6'}$ 7.67; $H_{3',5'}$ 7.49; $H_{4'}$ 7.40 $C_{2,6}$ 130,60; $C_{3,5}$ 127.78 $C_{2',6'}$ 127.37; $C_{3',5'}$ 129.81; $C_{4'}$ 128.45	7.2
Gln^4	8.17	4.05 55.80	2.05; 1.98 26.68	2.22 33.99		ε-NH_2 7.39; 6.78	3.4
Asn^5	8.34	4.70 n. o.	2.85 36.50			δ-NH_2 7.58; 6.89	3.9
Cys^6	7.98	n. o. n. o.	3.04; 281 38.99				3.2
Pro^7	-	4.38 n. o.	2.23; 1.85 29.99	1.94 25.49	3.61; 3.45 48.41		-
Arg^8	8.52	4.25 54.21	1.84; 1.74 28.69	1.62 25.12	3.15 41.25	ε-NH_2 7.12	8.8
Gly^9	8.35	3.88 42.90					6.1
C-NH_2	(E) 7.42 (Z) 7.03						-

n.o. – not observed

$H_\delta Pro^7$ indicates the *trans* geometry of this peptide bond. In the case of izomerization across a X-Pro peptide bond, the signals of C_β and C_γ of Pro are found at 30.5 ± 0.6 p.p.m. and at 25.1 ± 0.5 for the *trans* and at 32.2 ± 0.4 p.p.m. and 23.4 ± 0.3 for the *cis* isomer of each analogue obtained with EDMC and ANALYZE. Both the measured and computed vicinal couplings, $^3J_{HNH\alpha}$, of the peptides are shown in Table 7.

The lowest energy conformer of the [BPhe^3]AVP peptide forms β-turns at posi-

Table 2. Proton and carbon chemical shifts [p.p.m.] and the amide proton temperature coefficients [ppb/K] of the [BPhe^3, D-Arg^8]AVP peptide in water at 25°C

Residue	Chemical shift [ppm]						$-\Delta\delta/\Delta T$
	H_N	H_α	H_β	H_γ	H_δ	Others	[ppb/K]
Cys^1	n. o. n. o.	3.97 56.42	3.22; 3.04 41.57				n. o.
Tyr^2	n. o. n. o.	4.63 n. o.	2.95; 2.86 37.31			$H_{2,6}$ 7.03; $H_{3,5}$ 6.78 $C_{2,6}$ 131.17; $C_{3,5}$ 116.25	n. o.
BPhe^3	7.87	4.58 n. o.	3.24; 3.07 37.10			$H_{2,6}$ 7.23; $H_{3,5}$ 7.63 $H_{2',6'}$ 7.67; $H_{3',5'}$ 7.48; $H_{4'}$ 7.42 $C_{2,6}$ 130,63; $C_{3,5}$ 127.80 $C_{2',6'}$ 127.39; $C_{3',5'}$ 129.84; $C_{4'}$ 128.49	7.4
Gln^4	8.17	4.04 54.14	2.05; 1.98 26.84	2.20 32.17		ε-NH_2 7.39; 6.78	3.1
Asn^5	8.34	4.68 n. o.	2.85 36.66			δ-NH_2 7.58; 6.88	4.6
Cys^6	7.93	4.72 n. o.	2.99; 2.79 39.05				2.5
Pro^7	-	4.37 n. o.	2.23; 1.86 30.13	1.96 25.85	3.62; 3.48 48.99		-
D-Arg^8	8.60	4.26 55.00	1.88; 1.72 28.71	1.60 25.32	3.16 41.65	ε-NH_2 7.14	9.9
Gly^9	8.29	3.86 43.54					4.0
C-NH_2	(E) 7.30 (Z) 7.03						-

n.o. – not observed

(Dorman, 1973). The carbon chemical shifts of C_β and C_γ of Pro for all the peptides studied here indicate the *trans* Cys^6-Pro^7 peptide bond (Tables 1–3).

ANALYSIS OF THE STRUCTURES CALCULATED WITH EDMC AND ANALYZE

Tables 4, 5 and 6 summarize the statistical weights of the lowest energy conformations tions 3,4; 4,5 and 7,8 and a γ-turn at position 9. This γ-turn is stabilized by a hydrogen bond between the H_N proton of C-NH_2^9 and the oxygen atom of the carbonyl group of Arg^8. Two obtained conformations contain an inverse γ-turn at position 5, which is stabilized by appropriate hydrogen bonds.

The conformers found for the peptide [BPhe^3, D-Arg^8]VP contain mainly β-turns at positions 2,3; 3,4 and 4,5. Two of the obtained conformations have an inverse γ-turn at either position 2 or 5. The conformer with the

highest statistical weight forms a hydrogen bond between the H_N proton of Cys^6 and the side-chain of Asn^5.

In the peptide [Cpa^1, $BPhe^3$]AVP, a type I β-turn appears at position 2,3 in almost all obtained conformations. An inverse γ-turn at position 5 was found in the conformation with the highest statistical weight. The hydrogen bond between the H_N proton of Arg^8 and the carbonyl group of Cys^6 is populated.

A superposition of the conformations with the highest statistical weights for each peptide is presented in Fig. 3. The [Cpa^1, $BPhe^3$]AVP peptide reveals the smallest structural difference within this part of the molecule, with $RMSD_{1-6}$ of 0.963 Å for C_α.

ANALYSIS OF THE STRUCTURES CALCULATED USING THE X-PLOR PROGRAM

The final conclusion as to the secondary-structure elements present in each peptide will be drawn based on the calculations using inter-proton distances and torsion angles as constraints.

The conformations of each peptide were calculated and clustered into 49, 12 and 9 families of conformers for [$BPhe^3$]AVP, [$BPhe^3$]AVP and [Cpa^1, $BPhe^3$]AVP, respectively (Tables 4, 5 and 6). Only families consisting of two and more conformers were considered.

The lowest energy conformation of peptide [$BPhe^3$]AVP is stabilized by neither β-turns nor hydrogen bonds. In the case of the other structures of this peptide, the β-turn at position 3,4 appears most frequently. Two calculated conformations have a γ-turn at position 3, which is stabilized by the hydrogen bond between the H_N proton of Gln^4 and the carbonyl group of Tyr^2.

In the peptide [$BPhe^3$, D-Arg^8]VP a β-turn of type VII at position 4,5 was found for the lowest energy conformation. One obtained conformation possesses inverse γ-turns at positions 3 and 5. The hydrogen bond between H_N proton of Cys^6 and the carbonyl group of Gln^4 stabilizes the inverse γ-turn at position 5.

Table 3. Proton and carbon chemical shifts [ppm] and the amide proton temperature coefficients [ppb/K] of the [Cpa^1, $BPhe^3$]AVP peptide in water at 25°C

Residue	Chemical shift [ppm]						$-\Delta\delta/\Delta T$
	H_N	H_α	H_β	H_γ	H_δ	Others	[ppb/K]
Cpa^1	-	1.82 n. o.	-	1.49 35.39	1.37 22.79	H_ε 1.29 25.81	-
Tyr^2	7.73	4.42 n. o.	2.99; 2.82 35.57			$H_{2,6}$ 6.99; $H_{3,5}$ 6.77 $C_{2,6}$ 130.97; $C_{3,5}$ 116.18	n. o.
$BPhe^3$	7.45	n. o. n. o.	3.22; 3.15 37.42			$H_{2,6}$ 7.18; $H_{3,5}$ 7.53 $H_{2',6'}$ 7.61; $H_{3',5'}$ 7.38; $H_{4'}$ 7.27 $C_{2,6}$ 130,99; $C_{3,5}$ 127.32 $C_{2',6'}$ 127.23; $C_{3',5'}$ 129.66; $C_{4'}$ 128.37	n. o.
Gln^4	8.44	4.03 56.64	2.07 26.95	2.30 32.08		ε-NH_2 7.46; 6.83	4.1
Asn^5	8.39	4.60 n. o.	2.85 36.15			δ-NH_2 7.58; 6.89	6.8
Cys^6	7.87	4.37 52.93	2.85; 2.62 40.85				6.9
Pro^7	-	4.36 62.12	2.15 29.97	1.83 25.55	3.46; 3.18 49.05		-
Arg^8	8.20	4.25 54.64	1.83; 1.70 28.96	1.59 25.31	3.13 41.82	ε-NH_2 7.14	9.0
Gly^9	8.24	3.85 43.34					7.0
C-NH_2	(E) 7.40 (Z) 6.99						-

n.o. – not observed

In the case of peptide [Cpa[1], BPhe[3]]AVP, the lowest energy conformation has β-turns at positions 2,3 and 3,4. The majority of the calculated conformations form hydrogen bonds either between the H_N proton of Arg[8] and the carbonyl group of Cys[6] or the δH_N proton of Asn[5] and the carbonyl group of Gln[4]. No γ-turn was observed in those conformations.

COMPARISON OF THE RESULTS OBTAINED BY THE TWO CALCULATION METHODS

Figure 5 shows a comparison of the lowest energy conformations of each peptide obtained by the two different approaches, which reveals large structural differences with

Table 4. Statistical weights of the lowest energy conformations (with weights above 4%) obtained using EDMC and ANALYZE and the families of the low energy X-PLOR conformations from each family of the [BPhe[3]]AVP analogue in H_2O/D_2O at 25°C

EDMC and ANALYZE				XPLOR			
Positions and types of β-turns	H-bonds	Conformation number and geometry of SS bond	Pop. (%)	Positions and types of β-turns	H-bonds	Conformation number and geometry of SS bond	Number of conformations in each family cut=2.4 Å
3,4 β III 4,5 β IV 7,8 β III 9 γ	NH^2-CO^5 NH^9-CO^6 NH^{10}-CO^8	160 L	20.4	-	-	115 R	117
3,4 β I 4,5 β IV 5,6 β IV 7,8 β III	$NH^{5,6}$-CO^2 NH^6-CO^6	727 L	9.2	3,4 β II'	NH^4-CO^2	29 R	81
4,5 β I	NH^8-CO^6	683 L	9.2	3,4 β I 4,5 β I 5,6 β III 6,7 β I	NH^9-CO^7	256 R	31
3,4 β III 4,5 β III 5,6 β I 7,8 β III	NH^6-CO^2 NH^7-CO^3 NH^9-CO^6 NH^{10}-CO^7	276 R	7.6	2,3 β IV 3,4 β II' 5,6 β VII 3 γ 5 γ	NH^1-CO^2 NH^6-CO^4 NH^8-CO^6	23 L	10
4,5 β I	NH^8-CO^6	733 R	7.4	4,5 β IV	NH^8-CO^6	138 L	6
4,5 β I 7,8 β III 5 γ*	NH^6-CO^4	616 L	7.3	2,3 β IV 3,4 β I 6,7 β I	-	12 L	4
2,3 β III 5,6 β IV 7,8 β IV	-	896 R	5.7	2,3 β II 3,4 β IV 4,5 β II 6,7 β I 3 γ	NH^4-CO^1 NH^1-CO^2 NH^5-CO^3	244 R	3
4,5 β I 7,8 β IV 5 γ*	NH^6-CO^4	363 L	5.5	3,4 β II' 5,6 β IV	-	182 L	2
4,5 β I 7,8 β III 9 γ*	NH^9-CO^6 NH^{10}-CO^8	688 L	4.2	5,6 β III 6,7 β I	-	36 L	2
				3,4 β II' 4,5 β I 5,6 β IV	-	32 L	2
				2,3 β II 4,5 β II	NH^4-CO^1 NH^6-CO^1	262 R	2
				2,3 β II 3,4 β II' 4,5 β II 5,6 β III'	δNH^5-CO^4 NH^8-CO^6 NH^9-CO^7	295 R	2

L, left-handed disulfide bridge; R, right-handed disulfide bridge; γ*, inverse γ-turn

In all the analogues studied here, the largest variability of the backbone conformation is seen for the disulfide bridge, the Tyr[2] and BPhe[3] residues and the non-cyclic tail. A superposition of the lowest energy conformations for each peptide is presented in Fig. 4.

$RMSD_{1-6}$ = 1.483, 1.747 and 1.957 Å for C_α atoms, for peptides [BPhe[3]]AVP, [BPhe[3], D-Arg[8]]VP and [Cpa[1], BPhe[3]]AVP, respectively. These differences resulted from the specificity of the methods themselves. The structures obtained by the EDMC/ANALYZE

Table 5. Statistical weights of the lowest energy conformations (with weights above 7%) obtained using EDMC and ANALYZE and the families of the low energy X-PLOR conformations from each family of the [BPhe^3, D-Arg^8]VP analogue in H_2O/D_2O at 25°C

EDMC and ANALYZE				XPLOR			
Positions and types of β-turns	H-bonds	Conformation number and geometry of SS bond	Pop. (%)	Positions and types of β-turns	H-bonds	Conformation number and geometry of SS bond	Number of conformations in each family cut=2.4 Å
2,3 βIV 2 γ*	NH^6-δCO^5	226 L	22.7	4,5 βVII	-	69 R	251
3,4 βIII 4,5 βI 5,6 βI	$NH^{5,6}$-CO^2 NH^9-CO^7	257 R	12.4	2,3 βV 5 γ	NH^4-CO^2 NH^6-$CO^{3,4}$	220 R	35
2,3 βI 3,4 βI	-	117 L	11.4	3 γ* 5 γ*	NH^6-CO^4	216 R	3
2,3 βIII 3,4 βIV	NH^6-δCO^5	395 L	10.2	3,4 βIV 4,5 βVII 7,8 βV 8 γ	NH^8-CO^6 NH^9-CO^7	89 R	3
4,5 βI 5 γ*	NH^9-CO^7	240 L	8.4				
3,4 βIII	δNH^5-CO^6	330 L	7.8				

Table 6. Statistical weights of the lowest energy conformations (with weights above 8%) obtained using EDMC and ANALYZE and the families of the low energy X-PLOR conformations from each family of the [Cpa^1, BPhe^3]AVP analogue in H_2O/D_2O at 25°C

EDMC and ANALYZE				XPLOR			
Positions and types of β-turns	H-bonds	Conformation number and geometry of SS bond	Pop. (%)	Positions and types of β-turns	H-bonds	Conformation number and geometry of SS bond	Number of conformations in each family cut=2.4 Å
2,3 βIV 5,6 βIV 5 γ*	NH^6-CO^4	742 L	17.0	2,3 βIV 3,4 βVII	NH^8-CO^6	290 R	283
4,5 βI	NH^8-CO^6	416 L	14.9	4,5 βIV	δNH^5-CO^4	9 L	5
2,3 βIV	-	722 L	13.9	4,5 βVII 6,7 βI	δNH^5-CO^4 NH^8-CO^6	74 L	4
4,5 βIV	-	553 R	12.0	3,4 βIV 4,5 βI'	NH^6-CO^3 NH^8-εCO^4	280 L	2
2,3 βIII 3,4 βIV	NH^8-CO^6 NH^{10}-CO^7	758 R	11.8	4,5 βVII	-	222 L	2
2,3 βIII	NH^8-CO^6	741 L	8.7				

show a better fit between the NMR spectral evidence and the calculation for all the peptides. This is probably due to the fact that the computational method takes into account the conformational equilibrium of the peptides in solution as well as two parameters of considerable importance for short-chained peptides, namely the mixing and the correlation times. It is know that cyclic peptides tend to be more structured than linear ones, but they seldom have a single rigid conformation (Petsko, 1996). The numerous conformations in a dynamic exchange produce averaged NMR parameters and it is important that all available data be examined with caution (Walse *et al.*, 1998). In connection with this fact, the EDMC

Table 7. The measured and EDMC/ANALYZE computed values of the coupling constants, $^3J_{HNH\alpha}$ [Hz], of the peptides

Analogue / Residue	[BPhe^3]AVP		[BPhe^3, D-Arg^8]VP		[Cpa^1, BPhe^3]AVP	
	J_{exp}	J_{calc}	J_{exp}	J_{calc}	J_{exp}	J_{calc}
3	6.1	7.6	5.8	5.7		
4	3.9	5.7	3.8	6.2		
5	8.5	7.1	8.2	7.3	6.5	6.9
6	6.8	6.3	6.3	6.4		
8	7.0	5.9	7.5	6.2	6.1	5.8
9	5.9	6.5	5.9	6.3	5.5	6.0
Sd[a]	1.21443		1.19548		0.48323	

[a] Standard deviation in vicinal couplings

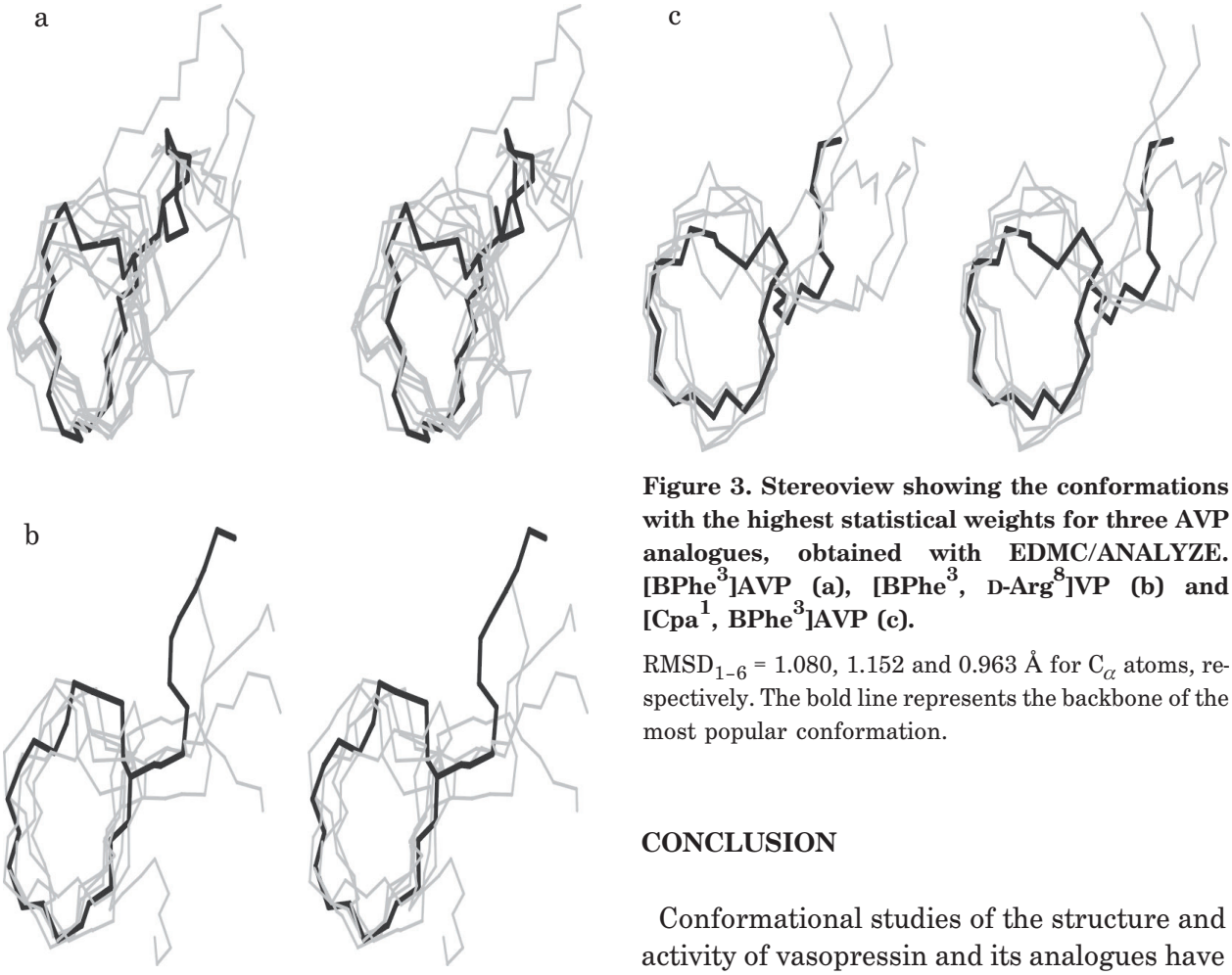

Figure 3. Stereoview showing the conformations with the highest statistical weights for three AVP analogues, obtained with EDMC/ANALYZE. [BPhe^3]AVP (a), [BPhe^3, D-Arg^8]VP (b) and [Cpa^1, BPhe^3]AVP (c).

$RMSD_{1-6}$ = 1.080, 1.152 and 0.963 Å for C_α atoms, respectively. The bold line represents the backbone of the most popular conformation.

method with the ECEPP/3 force field seems to be more suitable for short peptides, such as analogues of vasopressin.

CONCLUSION

Conformational studies of the structure and activity of vasopressin and its analogues have provided information on which of the functional groups in the sequence are responsible for the interaction with the cellular membrane receptors. It is know that positions 1, 2,

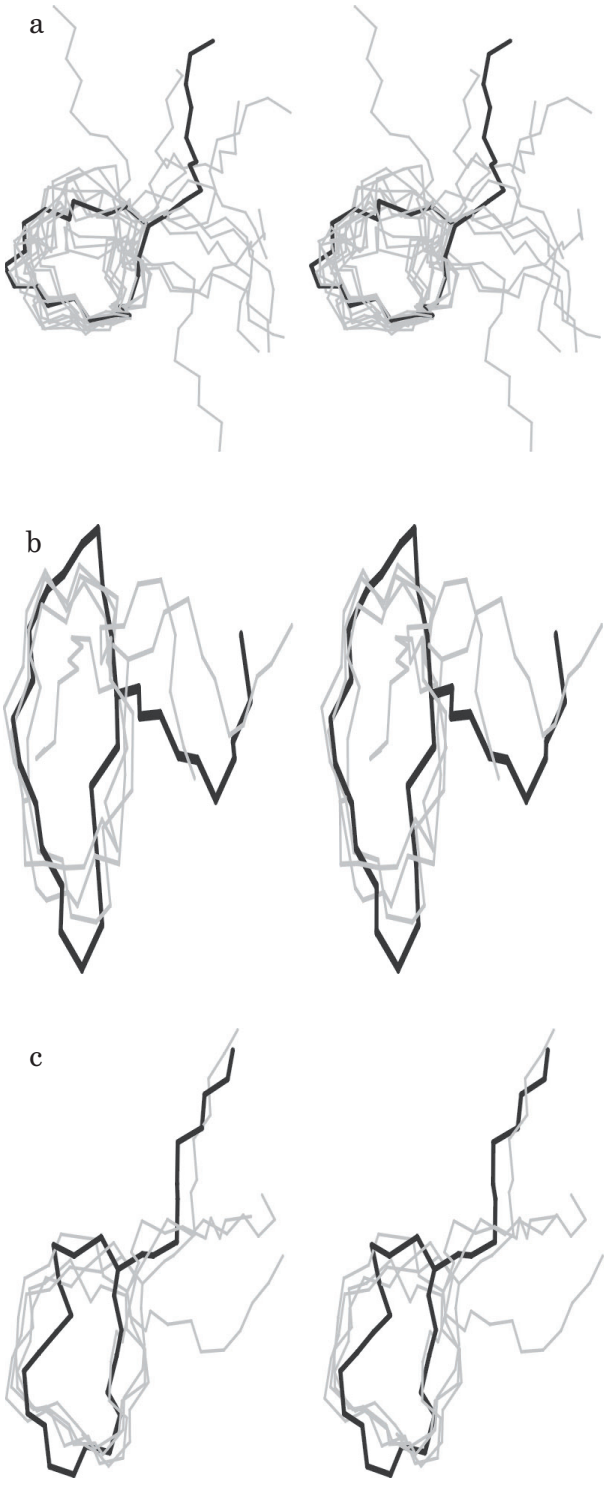

Figure 4. Stereoview showing the lowest energy conformations from each family for three AVP analogues obtained with XPLOR. [BPhe^3]AVP (a), [BPhe^3, D-Arg^8]VP (b) and [Cpa^1, BPhe^3]AVP (c).

$RMSD_{1-6}$ =1.221, 1.224 and 0.910 Å for C_α atoms, respectively. The bold line represents the backbone of the most popular conformation.

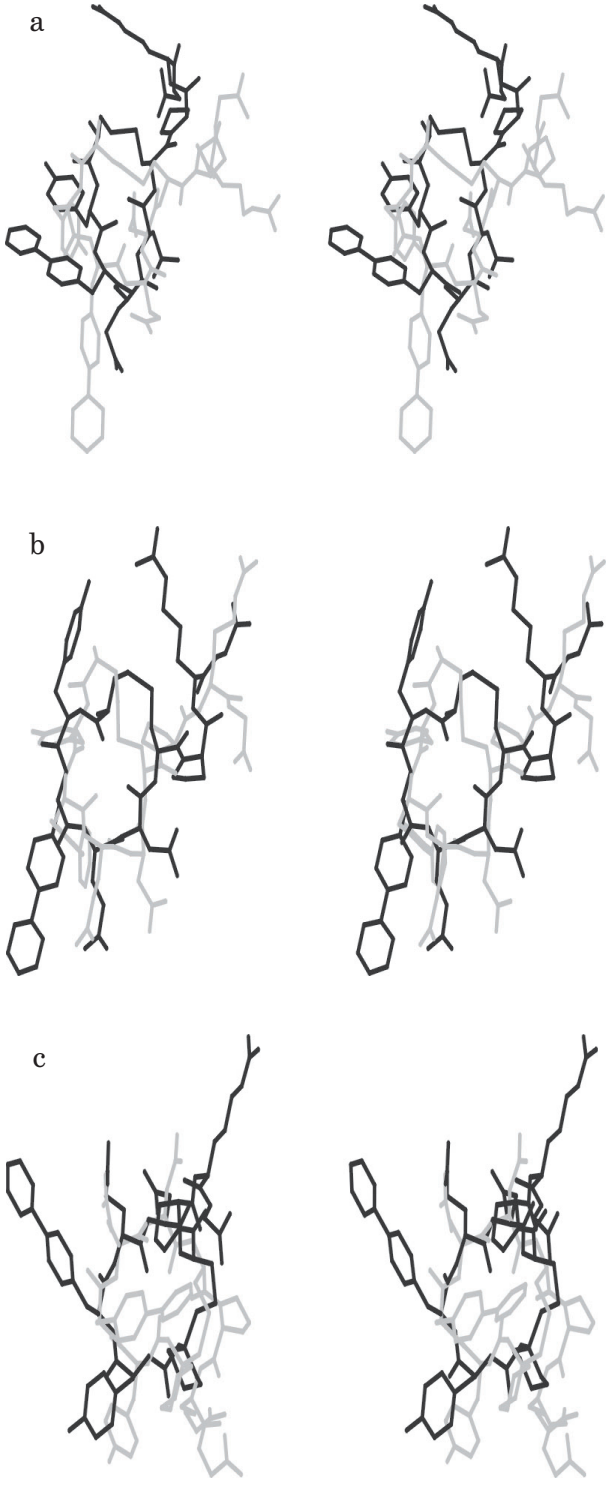

Figure 5. Stereoview of comparison of the lowest energy conformations obtained with EDMC/ANALYZE (black line) and X-PLOR (gray line), [BPhe^3]AVP (a), [BPhe^3, D-Arg^8]VP (b) and [Cpa^1, BPhe^3]AVP (c).

$RMSD_{1-6}$ =1.483, 1.747 and 1.370 Å for C_α atoms, respectively.

3 and 8 are crucial for antidiuretic activity, whereas the pressor activity is sensitive to changes at positions 1, 2, 8 and 9 (Manning *et al.*, 1987). The results of theoretical considerations on the interactions of AVP with lipids showed that only the side-chains of the Phe^3, Gln^4 and Pro^7 residues and the disulfide bridge interact with the phospholipid membrane, whilst the side-chains of Tyr^2, Asn^5, Arg^8 and Gly^9-NH_2 interact with the aqueous phase (Grzonka *et al.*, 1991). Additionally, a typical relaxed complex of V2R/AVP was generated by using modelling and computational methods (Czaplewski *et al.*, 1998). The results of that study showed that only the cyclic part vasopressin interacts with helices of the receptor, whilst the C-terminus is characterized by a considerable mobility.

The interaction of vasopressin with its receptors is determined by the correct orientation of some side-chains, including the side-chains of the residues in position 2 and 3.

In vasopressin, the orientation of Tyr^2 and Phe^3 side-chains is stabilized by a parallel π–π interaction between aromatic rings of these residues. Consequently, the side-chains of both aromatic residues extend away from the cyclic moiety. The greater hydrophobic properties of BPhe than Phe may be the reason for the change of interaction between the side-chains of the two neighbouring residues. As a result, the analogues with BPhe in position 3 are inactive, despite the fact that both aromatic residues lie outside the pressin ring as in vasopressin.

Conformational studies of native vasopressin in water (Hempel, 1987; Hruby & Lebl, 1987) and MeSO-d_6 (Schmidt *et al.*, 1991) have shown that its dominant structural features are β-turns within the Tyr^2-Asn^5 region. Similar results were obtained by computer-aided simulations of the [Arg^8]AVP molecule *in vacuo* (Liwo *et al.*, 1995; Kaźmierkiewicz *et al.*, 1997). Theoretical considerations revealed β-turns at positions 3,4 and 4,5. Also X-ray investigations of pressinoic acid (Langs *et al.*, 1986) revealed type II' and type I β-turns at positions 3,4 and 4,5, respectively. In the peptides studied by us, β-turns generally occur at a position between the second and fifth residue and at position 7,8. The non-cyclic part of each analogue is characterized by increased flexibility. Among the conformations of the presented peptides, the lowest energy conformer of [$BPhe^3$]AVP obtained with X-PLOR reveals a similar backbone and side-chain conformation of Gln^4 to the crystal structure of pressinoic acid. Furthermore, the Asn^5 side-chain lies over the molecule as in the case of pressinoic acid, in contrast to the Asn^5 in vasopressin which extends away from the cyclic part of the peptide (Skala *et al.*, 1984).

Analysis of the structures obtained with EDMC/ANALYZE reveals that the [$BPhe^3$]AVP and [$BPhe^3$, D-Arg^8] peptides contain β-turns of type I at position 4,5 in most conformations, similar to pressinoic acid.

REFERENCES

Bartles C, Xia T, Billeter M, Günter P, Wütrich K. (1995) The program XEASY for the computer-supported NMR spectral analysis of biological macromolecules. *J Biomol NMR.*; **5**: 1–10.

Bax A, Davis DG. (1985a) Practical aspects of two-dimensional transverse NOE spectroscopy. *J Magn Reson.*; **63**: 207–13.

Bax A, Freeman R. (1985b) Enhanced NMR resolution by restricting the effective sample volume. *J Magn Reson.*; **65**: 355–60.

Braunschweiler L, Ernst RR. (1983) Coherence transfer by isotropic mixing: Application to correlation spectroscopy. *J Magn Reson.*; **53**: 521–8.

Brooks B, Bruccoleri R, Olafson BO, States DJ, Swaminathan S, Karplus M. (1993) CHARMM: a program for macromolecular energy minimization and dynamics calculations. *Comp Chem.*; **4**: 187–17.

Brünger AT. (1993) *The X-PLOR Software Manual. Version 3.1*, Yale University Press, New Haven, CT.

Bystrov VF. (1976) Spin-spin coupling and the conformational states of peptide systems. *Progr NMR Spectrosc.*; **10**: 41–81.

Czaplewski C, Kaźmierkiewicz R, Ciarkowski J. (1998) Vasopressin V2 receptor/bioligand interactions. *Lett Peptide Sci.*; **5**: 333–5.

Dorman DE, Bovey FA. (1973) Carbon magnetic resonance spectroscopy. The spectrum of proline in oligopeptides. *J Org Chem.*; **38**: 2379–83.

Delaglio F, Grzesiek S, Geerten WV, Zhu G, Pfeifer J, Bax A. (1995) NMRPipe: a multidimensional spectral processing system based on UNIX pipes. *J Biomol NMR.*; **6**: 277–93.

Dyson HJ, Rance M, Hoighten RA, Lerner RA, Wright PE. (1988) Folding of immunogenic peptide fragments of proteins in water solution. I. Sequence requirements for the formation of a reverse turn. *J Mol Biol.*; **201**: 161–200.

Gottlieb HE, Kotlyar V, Nudelman A. (1997) NMR chemical shifts of common laboratory solvents as trace impurities. *J Org Chem.*; **62**: 7512–5.

Groth M, Malicka J, Czaplewski C, Liwo A, Łankiewicz L, Wiczk W. (1999) Maximum entropy approach to the determination of solution conformation of flexible polypeptides by global conformational analysis and NMR spectroscopy – application to DNS1-c[D-A2bu2, Trp4, Leu5]-enkephalin and DNS1-c[D-A2bu2, Trp4, D-Leu5]- enkephalin. *J Biomol NMR.*; **15**: 315–30.

Grzonka Z, Gwizdała E, Kasprzykowski F, Liwo A, Łankiewicz L, Łubkowska L, Galaktionov SG, Tseitin VM. (1991) Studies on the interaction of neurohypophyseal hormones with lipids. In *Peptides 90,* Giralt E, Andreu ,. eds, pp 488–9. ESCOM Science Publishers B.V., Leiden.

Güntert P, Wüthrich K. (1991) Improved efficiency of protein structure calculation from NMR data using program DIANA with redundant dihedral angle constraints. *J Biomol NMR.*; **1**: 447–56.

Güntert P, Braun W, Wüthrich K. (1991) Efficient computation of three-dimensional protein structures in solution from nuclear magnetic resonance data using the program DIANA and the supporting programs CALIBA, HABAS and GLOMSA. *J Mol Biol.*; **217**: 517–30.

Hempel JC. (1987) The conformation of neurohypophyseal hormones. In *The Peptides: Analysis, Synthesis, Biology*. Smith CW, eds, vol. 8, pp 209–37., Academic Press, New York.

Hlavacek J. (1987) Important structural modifications. Noncoded amino acid. In *Handbook of Neurohypophyseal Hormone Analogs.* Jošt K, Lebl M, Brtnik F, eds, vol. 1, pp 109–29. CRC Press Inc., Boca Raton, Florida.

Hruby VJ, Lebl MI. (1987) Conformational properties of neurohypophyseal hormone analogs in solutution as determined by NMR and laser RAMAN spectroscopies. In *Handbook of Neurohypophyseal Hormone Analogs.* Jošt K, Lebl M, Brtnik F. eds., pp. 105–55, vol. 1, CRC Press Inc., Boca Raton, Florida.

Kay LE, Keifer P, Saarinen T. (1992) Pure absorption gradient enhanced heteronuclear single quantum correlation spectroscopy with improved sensitivity. *J Am Chem Soc.*; **114**: 10663–5.

Kaźmierkiewicz R, Czaplewski C, Lammek B, Ciarkowski J. (1997) Molecular modeling of the neurophysin I/oxytocin complex. *J Comput Aided Mol Des.*; **11**: 9–20.

Kontaxis G, Stonehouse J, Laue ED, Keeler J. (1994) The sensitivity of experiments which use gradient pulses for coherence-pathway selection. *J Magn Reson Ser A.*; **111**: 70–6.

Koradi R, Billeter M, Wüthrich K. (1996) MOLMOL: a program for display and analysis of macromolecular structures. *J Mol Graphics.*; **14**: 52–5.

Koźminski W. (1998) The new active-coupling-pattern tilting experiment for an efficient and accurate determination of

homonuclear coupling constants. *J Magn Reson.*; **134**: 189–93.

Lammek B, Czaja M, Derdowska I, Łempicka E, Sikora P, Szkróbka W, Stojko R, Kupryszewski G. (1997) Influence of L-naphthylalanine in position 3 of AVP and its analogues on their pharmacological properties. *J Peptide Res.*; **49:** 261–8.

Langfeldt LA, Cooley ME. (2003) Syndrome of inappropriate antidiuretic hormone secretion in malignancy: review and implications for nursing management. *Clin J Oncol Nurs.*; **7**: 425–30.

Langs DA, Smith GD, Stezowski JJ, Hughes RE. (1986) Structure of pressinoic acid: the cyclic moiety of vasopressin. *Science.*; **232**: 1240–2.

László FA, László FJ, de Wied D. (1991) Pharmacology and clinical perspectives of vasopressin antagonists. *Pharmacol Rev.;* **43**: 73–108.

Lewis PN, Mamony FA, Sheraga HA. (1973) Chain reversals in proteins. *Biochim Biophys Acta.*; **303**: 211–29.

Liwo A, Tempczyk A, Oldziej S, Shenderovich MD, Hruby VJ, Talluri S, Ciarkowski J, Kasprzykowski F, Łankiewicz L, Grzonka Z. (1995) Exploration of the conformational space of oxytocin and arginine-vasopressin using the electrostatically driven Monte Carlo and molecular dynamics methods. *Biopolymers.*; **38**: 157–75.

Manning M, Balaspiri L, Moehring J, Haldar J, Sawyer WH. (1976) Synthesis and some pharmacological properties of deamino-(4-threonine, 8-D-arginine)vasopressin and deamino(8-D-arginine)vasopressin, highly potent and specific antidiuretic peptides, and (8-D-arginine)vasopressin and deamino-arginine-vasopressin. *J Med Chem.*; **19**: 842–5.

Manning M, Bańkowski K, Sawyer WH. (1987) Selective agonists and antagonists of vasopressin. In *Vasopressin*, Gash DW, Boer GJ, eds, pp 335–68. Plenum Publishing Corporation, New York.

Manning M, Cheng LL, Stoev S, Klis WA, Nawrocka E, Olma A, Sayer WH, Wo NC, Chan WY. (1997) Position three in vasopressin antagonist tolerates conformationally restricted and aromatic amino acid substitutions: a striking contrast with vasopressin agonists. *J Pept Sci.*; **3**: 31–46.

Marquard DW. (1963) An algorithm for least squares estimation of nonelinear parameters. *J Soc Industr Appl Math.*; **11**: 431–41.

Massefski WJr, Bolton PH. (1985) Quantitative analysis of nuclear Overhauser effects. *J Magn Reson.*; **65**: 526–30.

McDonald IK, Thornton JM. (1994) Satisfying hydrogen bonding potential in proteins. *J Mol Biol.;* **238**: 777–93.

Meadows RP, Post CB, Luxon BA, Gorenstein DG. (1994) *MORASS 2.1*. Purdue University, West Lafayette.

Némethy G, Gibson KD, Palmer KA, Yoon CN, Paterlini G, Zagari A, Rumsey S, Scheraga HA. (1992) Energy parameters in polypeptides. 10. Improved geometrical parameters and nonbonded interactions for use in the ECEPP/3 algorithm with application to proline-containing peptides. *J Phys Chem.*; **96**: 6472–84.

Palmer III AG, Cavanagh J, Wright PE, Rance M. (1991) Sensitivity improvement in proton-detected two dimensional heteronuclear correlation NMR spectroscopy. *J Magn Reson.*; **93**: 151–70.

Petsko GA. (1996) Not just your average structures. *Nat Struct Biol.;* **3**: 565–6.

Post CB, Meadows RP, Gorenstein DG. (1990) On the evaluation of interproton distance for 3-dimensional structure determination by NMR using a relaxation rate matrix analysis. *J Am Chem Soc.*; **112**: 6796–803.

Ripoll DR, Scheraga HA. (1988) On the multiple-minima problem in the conformational analysis of polypeptides. II. An electronically driven Monte Carlo method – tests on poly(L-alanine). *Biopolymers.*; **27**: 1283–303.

Schmidt JM, Ohlenschläger O, Rüterjans H, Grzonka Z, Kojro E, Pavo I, Fahrenholz F. (1991) Conformation of [8-arginine]vasopressin and V1 antagonists in dimethyl

sulfoxide solution derived from two-dimensional NMR spectroscopy and molecular dynamics simulation. *Eur J Biochem.*; **201**: 355–71.

Skala G, Smith CW, Taylor CJ, Ludens JH. (1984) A conformationally constrained vasopressin analog with antidiuretic antagonistic activity. *Science.*; **226**: 443–5.

Späth H. (1980) Cluster analysis algorithms. *J Comput Chem.*; **10**: 209–20.

Stoev S, Cheng LL, Olma A, Klis WA, Manning M, Wo NC, Chan WY. (1999) An investigation of position 3 in arginine vasopressin with aliphatic, aromatic, conformationally-restricted, polar and charged amino acids. *J Pept Sci.*; **5**: 141–53.

Vila J, Williams RL, Vsasquez M, Scheraga HA. (1991) Empirical solvation models can be used to differentiate native from near-native conformations of bovine pancreatic trypsin inhibitor. *Protein Struct Funct Genet.*; **10**: 199–218.

Walse B, Kihlberg J, Drakenberg B. (1998) Conformation of desmopressin, an analogue of the peptide hormone vasopressin, in aqueous solution as determined by NMR spectroscopy. *Eur J Biochem.*; **252**: 428–40.

Wishart DS, Bigam CG, Holm A, Hogdes RS, Sykes BD. (1995) 1H, 13C and 15N random coil NMR chemical shifts of the common amino acids. I. Investigations of nearest-neighbor effects. *J Biomol NMR.*; **5**: 67–81.

Wüthrich K, Billeter M, Braun W. (1983) Pseudo-structures for the 20 common amino acids for use in studies of protein conformations by measurements of intramolecular proton-proton distance constraints with nuclear magnetic resonance. *J Mol Biol.*; **169**: 949–61.

Wüthrich K, Billeter M, Braun W. (1984) Polypeptide secondary structure determination y nuclear magnetic resonance observation of short proton-proton distances. *J Mol Biol.*; **180**: 715–40.

Yu C, Yang TH, Yeh CJ, Chuang LC. (1992) Combined use of NMR, distance geometry, and restrained energy minimization for the conformational analysis of 8-lysinevasopressin. *Can J Chem.*; **70**: 1950–5.